

Research Article

Hole-Transporting Layer Treatment of Planar Hybrid n-Si/PEDOT:PSS Solar Cells with Power Conversion Efficiency up to 14.5%

Chenxu Zhang,¹ Yuming Zhang,¹ Hui Guo,¹ Zeyulin Zhang,² and Chunfu Zhang¹

¹Wide Bandgap Semiconductor Technology Disciplines State Key Laboratory, School of Microelectronics, Xidian University, Xi'an 710071, China

²School of Textiles and Materials, Xi'an Polytechnic University, Xi'an 710048, China

Correspondence should be addressed to Hui Guo; guohui@mail.xidian.edu.cn and Chunfu Zhang; cfzhang@xidian.edu.cn

Received 15 February 2017; Accepted 13 April 2017; Published 13 June 2017

Academic Editor: Pushpa Pudasaini

Copyright © 2017 Chenxu Zhang et al. This is an open access article distributed under the Creative Commons Attribution License, which permits unrestricted use, distribution, and reproduction in any medium, provided the original work is properly cited.

A systematical investigation was carried out into the effects of the hole-transporting layer treatment of poly(3,4-ethylenedioxythiophene):poly(styrenesulfonate) (PEDOT:PSS) on the performance of planar hybrid n-Si/PEDOT:PSS solar cells. Triton X-100 and ethylene glycol (EG) were chosen to improve the conductivity and surface morphology of the PEDOT:PSS film. It was found that the annealing temperature has a great influence on the PEDOT:PSS material properties and the corresponding device performance. By optimizing the annealing temperature, the conductivity of the PEDOT:PSS film doped with Triton X-100 and EG could be enhanced by a factor of more than three orders. And the corresponding device also shows record power conversion efficiency as high as 14.5% with an open circuit voltage of 0.627 V, a short circuit current of 32.6 mA/cm², and a fill factor of 70.7%.

1. Introduction

The solar cell is an efficient way to convert solar energy to electric power [1]. Presently, the mono- and multicrystalline silicon solar cells still dominate more than 90% of the PV market owing to their materials abundance and mature fabrication techniques. However, compared to the conventional energy sources, the cost of silicon solar cells is still too high because those devices are based on the p-n junctions which are generally formed by a high-temperature dopant diffusion process. Their high thermal budget accounts for ~30% of the total manufacturing cost of silicon (Si) solar cells [2]. To reduce the fabrication cost, the low-temperature solar cell concepts based on the organic/inorganic hybrid heterojunctions, particularly the Si/poly(3,4-ethylenedioxythiophene):poly(styrenesulfonate) (Si/PEDOT:PSS), have attracted significant research interest in recent years [3–6]. Si has a strong absorption ability in a very wide spectrum range and very excellent carrier transport ability. And PEDOT:PSS is a water-soluble polymer which has high conductivity, a

transmission window in the visible spectral range, and an excellent chemical and thermal stability [7]. This type of Si/PEDOT:PSS hybrid solar cell combines the superior absorption property of Si in a wide spectrum range and the advantage of aqueous solution-based processes for PEDOT:PSS [4], which avoids an expensive high-temperature process and promises a low-cost photovoltaic technique with the potential to realize a power conversion efficiency (PCE) as high as 22% in theory [5].

Since the first crystalline n-Si/PEDOT:PSS hybrid solar cell was reported in 2010 [4], great efforts, including the interface engineering [6, 8], treatment of PEDOT:PSS [9, 10], doping of the Si substrate [11], passivation on the device surface [12], nanoparticles [13, 14], and nanostructured surfaces [15–17], have been devoted to improve the device performance. Among these strategies, the treatment of the hole-transporting layer of PEDOT:PSS is a very simple and effective method.

Figure 1 shows the band structure of a hybrid Si/PEDOT:PSS cell concept, and it could be concluded that the

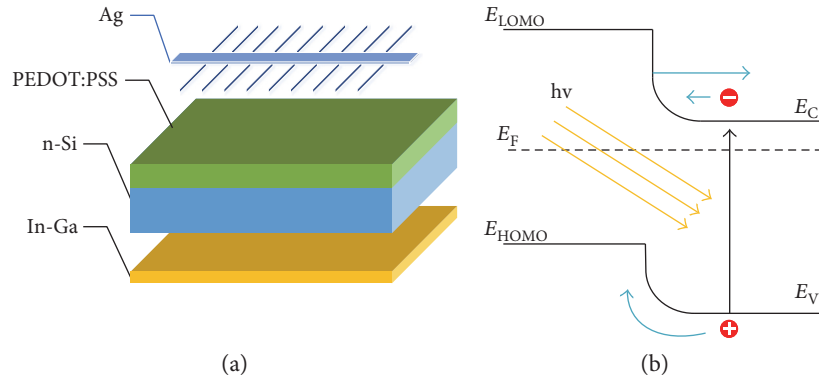


FIGURE 1: (a) Schematic structure of n-Si/PEDOT:PSS solar cell. (b) Schematic energy band diagrams of the device.

device performance greatly depends on the hole-conducting layer of PEDOT:PSS. Price et al. [18] made a comparison between hybrid Si/PEDOT:PSS heterojunctions and all-inorganic Si/Au Schottky junctions and found that the unfavorable electron injection rate from Si into PEDOT:PSS is three orders of magnitude smaller compared to that from Si into Au, which could result in high open circuit voltages (V_{OC}) in the corresponding device. Besides the interface properties, the holes must transport across the PEDOT:PSS layer before they could be collected by the electrode. Thus, the material properties of PEDOT:PSS could greatly affect the device characteristics [18].

The basic building block of PEDOT is thiophene. By adding stabilizing side groups, this material has a high thermal and chemical stability. Its conductivity could be enhanced by oxidizing the thiophene backbone with sodium peroxodisulfate, and thus, the polymer characteristics could be converted from a chromophoric to a metallic behavior. Recent results have shown that the additive in the liquid state may provide space for the reorientation of PEDOT:PSS chains [19] and is important for further conductivity enhancement. Several methods have been reported to enhance the conductivity of PEDOT:PSS. Kim et al. reported that addition of a high dielectric solvent into an aqueous solution of PEDOT:PSS can enhance the conductivity of the resulting PEDOT:PSS film by more than one order of magnitude as a result of weakening of the coulombic attraction between the counter ions and the charge carriers [20]. Sorbitol, ethylene glycol (EG), and other alcohols comprise another set of inert secondary dopants that can enhance the conductivity [20]. The exact principle of the enhancement has not been recognized, and several mechanisms have been proposed. It is generally believed that the solvent optimizes the morphology of the films, providing good percolating paths among the PEDOT:PSS domains (PEDOT-rich regions) and transforming the molecular structure. Xia et al. proposed that the additive does not only act simply as a plasticizer but also change the conformation in the PEDOT:PSS film [4]. All these studies mainly focused on the material properties instead of their influence on the solar cells. However, compared to the many reports about the material researches about the conductivity modulation of PEDOT:PSS, the systematic studies about the treatment of

PEDOT:PSS on the corresponding performance of hybrid Si/PEDOT:PSS cell are still lacking.

The aim of the current study is to systematically investigate the effects of the hole-transporting layer treatment of PEDOT:PSS on the performance of planar hybrid n-Si/PEDOT:PSS solar cells. In this work, the conductivity and surface morphology of PEDOT:PSS film were improved by adding the Triton and EG in the aqueous PEDOT:PSS solution. It was found that the annealing temperature has a great influence on the PEDOT:PSS material properties and the corresponding device performance. By optimizing the annealing temperature, the conductivity of the PEDOT:PSS film doped with Triton and EG could be enhanced by a factor of more than three orders. And the corresponding device also shows a recorded PCE as high as 14.5% with a V_{OC} of 0.627 V, a short circuit current (J_{SC}) of 32.6 mA/cm², and a fill factor (FF, the ratio of maximum obtainable power to the product of V_{OC} and J_{SC}) of 70.7%.

2. Experimental

2.1. Film Formation and Device Fabrication. n-type Si/PEDOT:PSS hybrid heterojunction solar cells were fabricated on the sequence below: n-type Si (100) wafers with a thickness of 300 μm and a resistivity of 0.05–0.1 $\Omega\text{-cm}$ was cut into $1.5 \times 1.5 \text{ cm}^2$ for solar cell fabrication and ultrasonically cleaned in acetone, isopropyl alcohol, and ionized water sequentially for 10 min. The native oxide on the silicon surface (about 4 nm) was etched by dipping the sample into hydrofluoric acid (5% HF for 30 s) and then drying by N_2 for later use. In order to improve wettability and to form a uniform PEDOT:PSS film on a Si substrate, Triton X-100 is added as a surfactant. PEDOT:PSS (PH1000, Heraeus Clevios) was filtered with polyvinylidene fluoride membrane (0.45 μm porosity) to remove agglomerations. To increase the conductivity of the PEDOT:PSS film, the optimized 7 vol% EG were added to the PEDOT:PSS solution and Triton X-100 (1%) was then added to it. The solution was spin coated on the HF-treated Si substrate at a speed of 2500 rpm for 60 s. The samples were annealed on a hot plate at 190°C for 15 min to remove the solvent to form a uniform and conductive p-type organic thin film. A 150 nm thick Ag film was thermally evaporated to form a grid. Finally, the

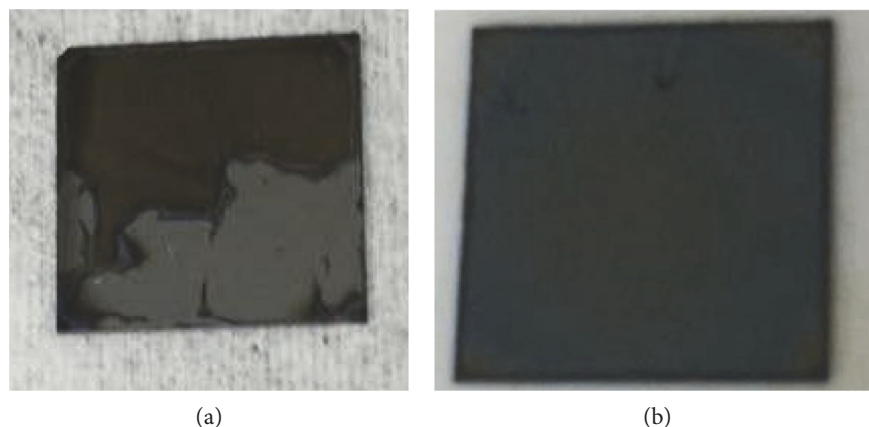


FIGURE 2: Photos (a) before and (b) after Triton X-100 treatment.

eutectic In-Ga fully covered the rear side of the Si substrates to form an ohmic contact.

2.2. Device Characterization. The morphology measurements of the PEDOT:PSS films was measured by atomic force microscopy (AFM). The UV-visible reflection spectra were recorded with UV-visible spectrophotometer (Perkin-Elmer Lambda 950). Photovoltaic parameters were measured by using a Keithley 2400 source meter under simulated sunlight from XES-70S1 solar simulator matching the AM 1.5G standard with an intensity of 100 mW/cm^2 . The system was calibrated against a NREL-certified reference solar cell. All the measurements of the solar cells were performed under ambient atmosphere at room temperature without any encapsulation.

3. Results and Discussion

The n-Si/PEDOT:PSS hybrid solar cell is structured as In-Ga eutectic/n-Si/PEDOT:PSS/Ag as shown in Figure 1(a). There is a type III hybrid interface between Si and PEDOT:PSS as shown in Figure 1(b). The device operation is based on a charge-selective interface, where the PEDOT:PSS and the n-Si act as hole- and electron-transport layers, respectively. Lights are illuminated from the top of the cell, where the PEDOT:PSS film is more than 90% transparent at such a thickness in the visible spectral range. Therefore, most of the light is absorbed by n-Si. Due to the high conductivity of the PEDOT:PSS layer, a depletion region in Si near the interface of n-Si/PEDOT:PSS is formed. As shown in Figure 1(b), the LOMO level of the PEDOT:PSS is much higher than the conductance band of the n-Si, so the electrons under illumination would be blocked from flowing into the PEDOT:PSS layer. On the other hand, the HOMO level of PEDOT:PSS is closely aligned with the valence band of n-Si, allowing holes in the n-Si to flow into the PEDOT:PSS film. The depletion region separates the photogenerated carriers in n-Si to the opposite direction, which suggests that electrons can be transported to the rear side of the n-Si and collected by the cathode. At the same time, the holes are transported to the anode through the PEDOT:PSS layer.

The thickness of the PEDOT:PSS film was measured by AFM and found to be about 55 nm.

The silicon surface has highly hydrophobic properties after etching by HF solution. It is not easy to form a uniform PEDOT:PSS film on such a surface by spin coating the aqueous PEDOT:PSS solution. To overcome this problem and ensure proper wetting of PEDOT:PSS on the Si substrates, Triton X-100 is added in the PEDOT:PSS solution. Figures 2(a) and 2(b) show the pictures of PEDOT:PSS films before and after the addition of Triton X-100. The PEDOT:PSS film without Triton addition was quite rough and cannot cover all of the substrate. By adding the Triton X-100, the adhesion of PEDOT:PSS conjugated polymer on hydrophobic n-Si has been improved, resulting in an efficient suppression of defect generation at the n-Si/PEDOT:PSS interface.

In order to improve the conductivity of the PEDOT:PSS films, EG is chosen to be added in the aqueous PEDOT:PSS solution since it can improve the electrical conductivity due to phase separation of the hydrophilic conductive PEDOT and the hydrophobic insulating PSS, which leads to an increase in the hole mobility. Figure 3(a) shows J - V characteristics of the fabricated n-Si/PEDOT:PSS cells. All the devices were fabricated by the same procedures except for the different annealing temperatures. DMSO is also added in the aqueous PEDOT:PSS solution as the reference and its device parameters is summarized in Table 1. In solar cells, where the PEDOT:PSS films are doped by DMSO-Triton (100:5 v/v), EG-Triton (100:7 v/v) is represented as the DMSO cell and EG cell. The J - V characteristics of PV cells can be approximately described by the Shockley equation

$$J = J_0 \left(\exp \left(\frac{q(V - R_s J)}{nk_B T} \right) - 1 \right) + \frac{V - R_s J}{R_{sh}} - J_{ph}, \quad (1)$$

where J_0 is the saturation current, J_{ph} the photocurrent, R_s the series resistance, R_{sh} the shunt resistance, n the ideality factor, q the electron charge, k_B the Boltzmann constant, and T the temperature. By using (1) with our proposed explicit analytic expression method [21], the experimental data can be well rebuilt as shown in Figure 3(a), which

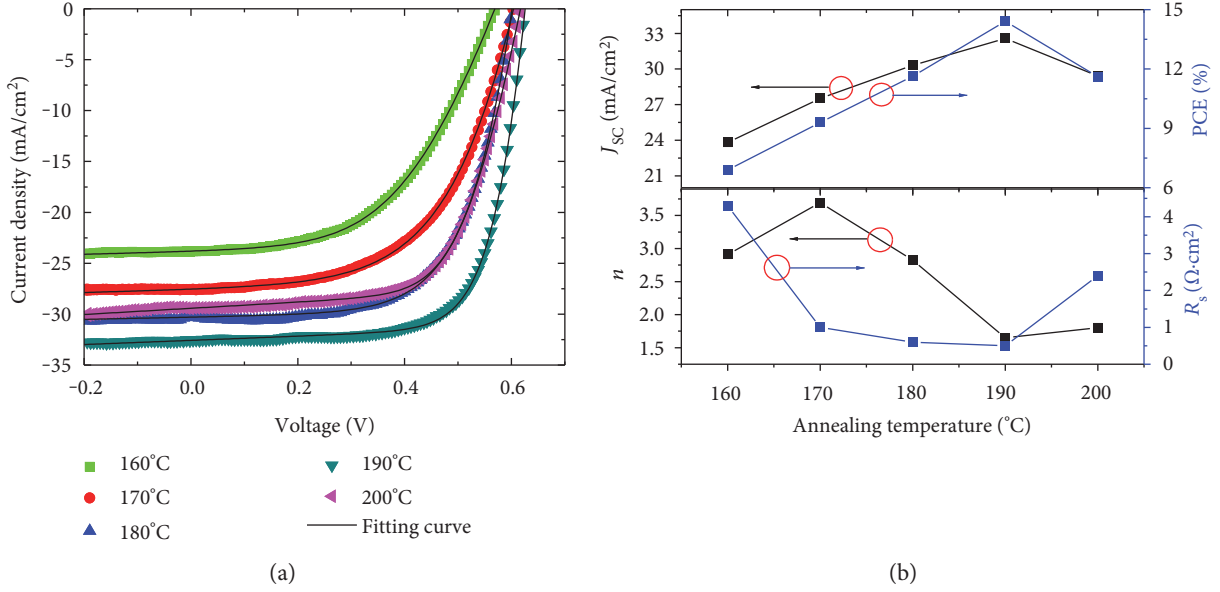


FIGURE 3: (a) Illuminated J - V characteristics of the solar cells annealing on different temperatures. The J - V experimental data are fit by (1). (b) The cells' parameters with different annealing temperatures.

TABLE 1: Photovoltaic performance of n-Si/PEDOT:PSS solar cells under AM 1.5G illumination (100 mW/cm²).

	V_{oc} (V)	J_{sc} (mA/cm ²)	FF (%)	PCE (%)
DMSO cell	0.598	25.6	57.4	8.8
EG cell 160	0.569	23.8	50.9	6.9
EG cell 170	0.604	27.5	55.9	9.3
EG cell 180	0.602	30.3	63.8	11.6
EG cell 190	0.627	32.6	70.7	14.5
EG cell 200	0.617	29.4	64.0	11.6

confirmed the validity of the extracted parameters. Table 1 summarizes the device performance parameters. The device with the DMSO addition exhibits a J_{SC} of 25.6 mA/cm², a V_{OC} of 0.598 V, and a FF of 57.4%, leading to a corresponding PCE of 8.8%, and its performance is relatively constant with different annealing temperatures. The performance is comparable to the reported results with a similar device structure [19]. It is obvious that the low J_{SC} is the main factor that limits the PCE. Compared with the DMSO cells, the EG cells have significantly improved in performance with a proper annealing temperature as shown in Figures 3(a) and 3(b). When the annealing temperature is 160°C, the performance of the device is low with a J_{SC} of 23.8 mA/cm², a V_{OC} of 0.569 V, and a FF of 50.9%, resulting in a PCE of 6.9%. With the increase of the annealing temperature, all of J_{SC} , V_{OC} , and FF improved. When the annealing temperature is 190°C, the optimized device is achieved. J_{SC} increased to 32.6 mA/cm², V_{OC} increased to 0.627 V, FF increased to 70.7%, and the overall PCE improved to 14.5%. It is inferred that the EG can help enhance the uniformity and conductivity of PEDOT:PSS film with a proper annealing temperature

and thus improve the device performance. Beyond 190°C, the device performance decreased with a higher annealing temperature. From Figure 3(b), it also could be seen that the annealing temperature could greatly affect the ideality factor and the series resistance. When the annealing temperature is 160°C, n is 2.91 and R_s is 4.3 Ω·cm⁻². When the annealing temperature is increased to 190°C, n decreases to 1.65 and R_s is 0.5 Ω·cm⁻², which means that an optimized annealing temperature could greatly improve the conductivity of the hole-transporting layer and thus enhance the device performance. The reason maybe that proper temperature could evaporate the water of the PEDOT:PSS solvent as well as have a positive effect in PEDOT:PSS chain reforming to a high conductive state. The conductivity measurement also shows that the optimized annealing temperature could enhance the conductivity of the PEDOT:PSS film with Triton and EG addition from 0.2 to over 200 S/cm, and this is consistent with the J - V characteristics of the hybrid solar cells. The same trend of the influence of annealing temperature on the hybrid GaN/PEDOT:PSS solar cells is also reported in one previous work [22]. It is shown that the annealing could affect the work function and conductivity of PEDOT:PSS. XPS measurements and J - V characteristics analysis indicate that the change of the V_{OC} can be due to the work function variations of the PEDOT:PSS and the barrier height of the Schottky contact, while the change of the J_{SC} can be ascribed to the competition between the enhancement of the conductivity and the thermal degradation of the PEDOT:PSS. Thus, there is an optimized annealing temperature so that almost all the device parameters could be improved. For our case, the optimized annealing temperature is 190°C.

Figure 4 shows AFM images of PEDOT:PSS films annealed at different annealing temperatures and their corresponding root-mean-square (RMS) value variation with the different annealing temperatures. When the annealing

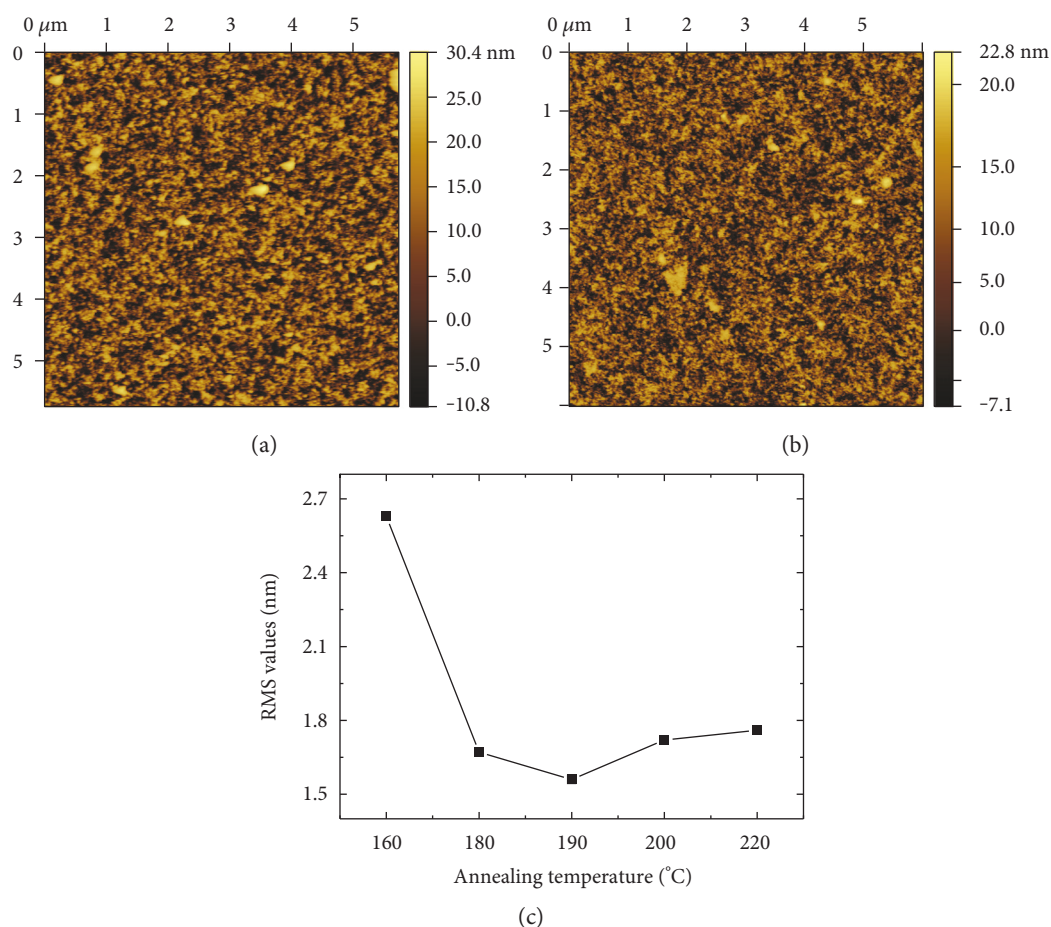


FIGURE 4: AFM images of PEDOT:PSS films annealed at (a) 160°C and (b) 190°C. (c) RMS value variation of PEDOT:PSS films with the different annealing temperatures.

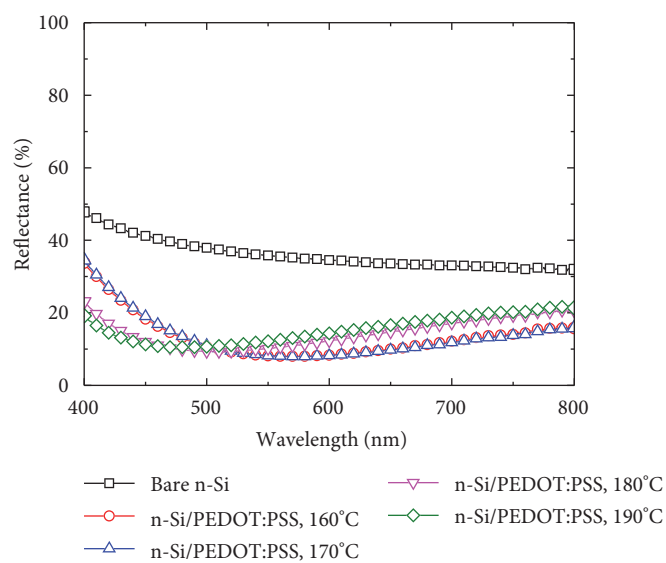


FIGURE 5: Reflectance spectra of n-Si/PEDOT:PSS samples annealed at different temperatures from 160°C to 190°C, and the reflectance spectrum of the polished bare n-Si is also shown for a reference.

temperature is 160°C, a relatively rough surface of PEDOT:PSS film is obtained with a root-mean-square (RMS) value of 2.63 nm as shown in Figure 4(a). For the optimized annealing temperature of 190°C, a relatively smooth surface is obtained with a RMS value of 1.56 nm as shown in Figure 4(b). The annealing temperature could greatly affect the roughness of PEDOT:PSS films. The variation of RMS values with different annealing temperatures as shown in Figure 4(c) matched the performance variation of devices as shown in Figure 3(b). A uniform hole-transparent layer could suppress the recombination on the junction and promote the hole current by enhancing the carrier collection ability. This may be one reason for the higher device performance annealed at the optimized temperature of 190°C.

We also investigate how the annealing temperature affects the optical properties of n-Si/PEDOT:PSS structures by measuring the reflectance spectra. Figure 5 shows the variation of the reflectance spectra of n-Si/PEDOT:PSS structures with the annealing temperatures from 160°C to 190°C. The reflectance spectrum of the polished bare n-Si is also shown in Figure 5 for a reference. The planar polished bare n-Si exhibits a reflectance of more than 30% over a wavelength range from 400 nm to 800 nm, while all the samples with n-Si/PEDOT:PSS structures show a reduced reflectance. This means that the PEDOT:PSS film could help to improve the overall light absorption ability. Comparing the samples with n-Si/PEDOT:PSS structures annealed at different temperatures, it could be found that the sample with the 190°C annealing temperature shows a relatively larger reflectance compared to the sample with a relatively low annealing temperature such as 160°C for the wavelength range from 500 nm to 800 nm. This means that there is no absorption improvement for the device with the 190°C annealing temperature. The enhanced device performance for the optimized annealing temperature of 190°C should result from the improved carrier collection ability instead of the absorption improvement. The device performance could be further improved by enhancing the optical absorption ability with the antireflective film or the textured Si surface.

4. Conclusion

In summary, doping PEDOT:PSS with EG and Triton is an effective method to improve the conductivity of PEDOT:PSS films and at the same time there is great influence of the annealing temperature on the final film properties. The proper annealing temperature could improve the film morphology, increase the film conductivity, and decrease the device series resistance. Compared with the devices with the different annealing temperatures, the planar hybrid Si/PEDOT:PSS solar cell annealed at 190°C shows the optimized performance and PCE reaches as high as 14.5% with a J_{SC} of 32.6 mA/cm², a V_{OC} of 0.627 V, and a FF of 70.7%. A further improvement is expected by enhancing the optical absorption ability with the antireflective film or the textured Si surface.

Conflicts of Interest

The authors declare that there is no conflict of interest regarding the publication of this paper.

Acknowledgments

The authors thank the Natural Science Foundation of China (61604119), Young Talent fund of University Association for Science and Technology in Shaanxi, China (20150103), Fundamental Research Funds for the Central Universities (Grant nos. JB151406, JB161101, and JB161102), and class general financial grant from the China Postdoctoral Science Foundation (Grant no. 2016M602771).

References

- [1] W. Hoffmann, "PV solar electricity industry: market growth and perspective," *Solar Energy Materials & Solar Cells*, vol. 90, no. 18, pp. 3285–3311, 2005.
- [2] S. B. Darling, "Block copolymers for photovoltaics," *Energy Environment Science*, vol. 2, no. 12, pp. 1266–1273, 2009.
- [3] S. C. Shiu, J. J. Chao, S. C. Hung, C. L. Yeh, and C. F. Lin, "Morphology dependence of silicon nanowire/poly(3,4-ethylenedioxythiophene):poly(styrenesulfonate) heterojunction solar cells," *Chemistry of Materials*, vol. 22, no. 10, pp. 3108–3113, 2010.
- [4] Y. Xia, H. Zhang, and J. Ouyang, "Highly conductive PEDOT : PSS films prepared through a treatment with zwitterions and their application in polymer photovoltaic cells," *Journal of Materials Chemistry*, vol. 20, no. 43, pp. 9740–9747, 2010.
- [5] J. Sheng, K. Fan, D. Wang et al., "Improvement of the SiO_x passivation layer for high-efficiency Si/PEDOT:PSS heterojunction solar cells," *ACS Applied Materials & Interfaces*, vol. 6, no. 18, pp. 16027–16034, 2014.
- [6] S. Jäckle, M. Liebhaber, J. Niederhausen et al., "Unveiling the hybrid n-Si/PEDOT:PSS interface," *ACS Applied Materials & Interfaces*, vol. 8, no. 13, pp. 8841–8848, 2016.
- [7] L. Groenendaal, F. Jonas, D. Freitag, H. Pielartzik, and J. R. Reynolds, "Poly (3, 4-ethylenedioxythiophene) and its derivatives: past, present, and future," *Advanced Materials*, vol. 12, no. 7, pp. 481–494, 2000.
- [8] M. Pietsch, S. Jackle, and S. Christiansen, "Interface investigation of planar hybrid n-Si/PEDOT:PSS solar cells with open circuit voltages up to 645 mV and efficiencies of 12.6%," *Applied Physics A: Materials Science & Processing*, vol. 115, no. 4, pp. 1109–1113, 2014.
- [9] J. Ouyang, Q. Xu, C. W. Chu, Y. Yang, G. Li, and J. Shinar, "On the mechanism of conductivity enhancement in poly(3,4-ethylenedioxythiophene):poly(styrene sulfonate) film through solvent treatment," *Polymer*, vol. 45, no. 25, pp. 8443–8450, 2004.
- [10] C. S. Pathak, J. P. Singh, and R. Singh, "Effect of dimethyl sulfoxide on the electrical properties of PEDOT:PSS/n-Si heterojunction diodes," *Current Applied Physics*, vol. 15, no. 4, pp. 528–534, 2015.
- [11] S. Jäckle, M. Mattiza, M. Liebhaber et al., "Junction formation and current transport mechanisms in hybrid n-Si/PEDOT:PSS solar cells," *Scientific Reports*, vol. 5, article 13008, 2015.
- [12] P. Yang, D. Xie, Y. Zhao et al., "NO₂-induced performance enhancement of PEDOT:PSS/Si hybrid solar cells with a high

- efficiency of 13.44%," *Physics Chemical Chemical Physics*, vol. 18, no. 10, pp. 7184–7189, 2016.
- [13] T. Song, S. T. Lee, and B. Sun, "Prospects and challenges of organic/group IV nanomaterial solar cells," *Journal of Materials Chemistry*, vol. 22, no. 10, p. 4216, 2010.
- [14] Z. Xia, T. Song, J. Sun, S. T. Lee, and B. Sun, "Plasmonic enhancement in hybrid organic/Si heterojunction solar cells enabled by embedded gold nanoparticles," *Applied Physics Letters*, vol. 105, no. 24, pp. 18–22, 2014.
- [15] K. T. Park, H. J. Kim, M. J. Park et al., "13.2% efficiency Si nanowire/PEDOT:PSS hybrid solar cell using a transfer-imprinted Au mesh electrode," *Scientific Reports*, vol. 5, article 12093, 2015.
- [16] L. He, Rusli, D. Lai, and H. Wang, "Highly efficient Si-nanorods/organic hybrid core-sheath heterojunction solar cells," *Applied Physics Letters*, vol. 99, no. 2, pp. 3–6, 2011.
- [17] S. Jeong, E. C. Garnett, S. Wang et al., "Hybrid silicon nanocone-polymer solar cells," *Nano Letters*, vol. 12, no. 6, pp. 2971–2976, 2012.
- [18] M. J. Price, J. M. Foley, R. A. May, and S. Maldonado, "Comparison of majority carrier charge transfer velocities at Si/polymer and Si/metal photovoltaic heterojunctions," *Applied Physics Letters*, vol. 97, no. 8, article 83503, 2010.
- [19] M. Pietsch, M. Y. Bashouti, and S. Christiansen, "The role of hole transport in hybrid inorganic/organic silicon/poly(3,4-ethylenedioxy-thiophene): poly(styrenesulfonate) heterojunction solar cells," *The Journal of Physical Chemistry C*, vol. 117, no. 18, pp. 9049–9055, 2013.
- [20] J. Y. Kim, J. H. Jung, D. E. Lee, and J. Joo, "Enhancement of electrical conductivity by a change of solvents," *Synthetic Metals*, vol. 126, no. 2, pp. 311–316, 2002.
- [21] C. Zhang, J. Zhang, Y. Hao, Z. Lin, and C. Zhu, "A simple and efficient solar cell parameter extraction method from a single current-voltage curve," *Journal of Applied Physics*, vol. 110, no. 6, Article ID 064504, 2011.
- [22] Q. Feng, K. Du, Y. Li, P. Shi, and F. Qing, "Effect of annealing on performance of PEDOT:PSS/n-GaN Schottky solar cells," *Chinese Physics B*, vol. 23, no. 7, article 077303, 2014.

